

## Supporting information

### Free-standing films of nickel nanowires anchored with Ni<sub>3</sub>S<sub>2</sub> nanosheets for stable Li anodes

Yang Xu, Gang Li, Jiangtao Hai, Hwei Yuan, Haotian Weng, Kun Li, Xiaolu Huang, Yanjie Su,  
Nantao Hu\*, Yafei Zhang\*

Department of Micro/Nano Electronics, School of Electronics, Information and Electrical  
Engineering, Shanghai Jiao Tong University, Shanghai 200240, P. R. China

\* Corresponding authors

hunantao@sjtu.edu.cn (Nantao Hu) and yfzhang@sjtu.edu.cn (Yafei Zhang)

### *Computational details*

In this study, we employed the Vienna Ab initio Simulation Package (VASP) to conduct all simulations based on Density Functional Theory (DFT). Exchange-correlation energies were calculated using the Generalized Gradient Approximation (GGA), as developed by Perdew, Burke, and Ernzerhof (PBE)<sup>S1, 2</sup>. Core ions were modeled using the Projected Augmented Wave (PAW) method, and valence electrons were expanded using a plane wave basis set with an energy cutoff of 520 eV. To accurately describe van der Waals interactions, crucial for the adsorption process, we applied the rev-vdW-DF2 correction<sup>S3, 4</sup>. We optimized the Brillouin zone sampling with a k-mesh grid of  $5 \times 5 \times 1$  to balance computational efficiency with the required precision for slab model. The convergence criterion for electronic states was defined by a total energy change less than  $10^{-6}$  eV between iterations. Gaussian smearing, with a width of 0.05 eV, was used to manage partial occupancies in the Kohn-Sham orbitals. The geometry optimization convergence threshold was set when atomic forces were reduced to below 0.02 eV/Å. To compute the adsorption energies of Li atoms on Ni (111) and Ni<sub>3</sub>S<sub>2</sub> (-110) surfaces, we used the following formula:

$$E_{ads} = E_{Li/surface} - (E_{surface} + E_{Li}) \quad (S1)$$

where  $E_{ads}$  denotes the adsorption energy of a Li atom on a specific surface.  $E_{Li/surface}$  is the total energy of the system with the Li atom adsorbed,  $E_{surface}$  is the energy of the clean surface (either Ni (111) or Ni<sub>3</sub>S<sub>2</sub> (-110)), and  $E_{Li}$  represents the energy of a Li atom in its bulk state. This formula is crucial for analyzing the energetic aspects of the adsorption process, providing insights into the stability and migration patterns of Li atoms on these surfaces.

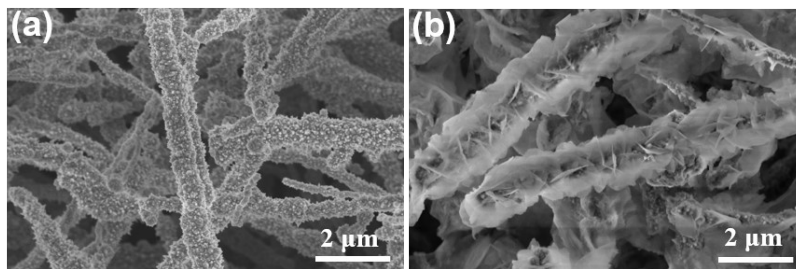


**Fig. S1.** SEM images of (a) NiNWs and (b) NiNWs@Ni<sub>3</sub>S<sub>2</sub> at low magnification.

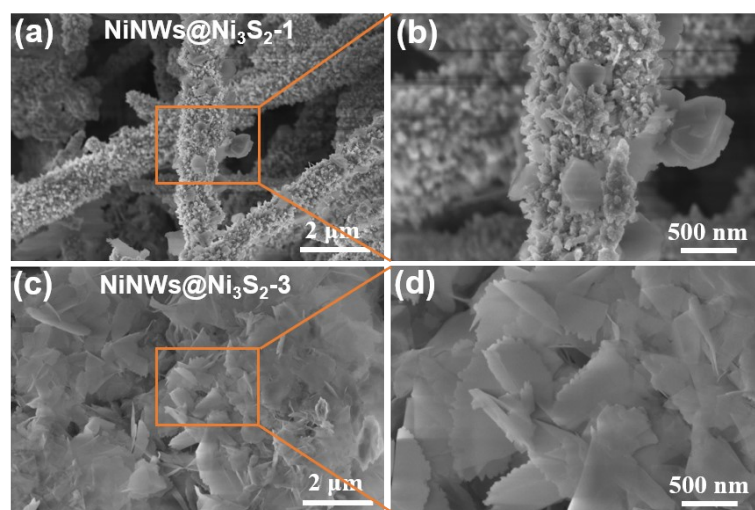


**Fig. S2.** SEM images at different magnifications for (a, b) NiNWs@Ni<sub>3</sub>S<sub>2</sub>-1 and (c, d) NiNWs@Ni<sub>3</sub>S<sub>2</sub>-3.

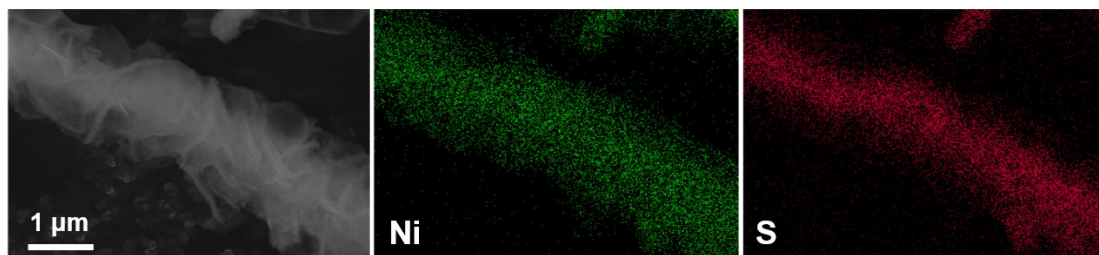


**Fig. S3.** Elemental mapping of NiNWs@Ni<sub>3</sub>S<sub>2</sub>.

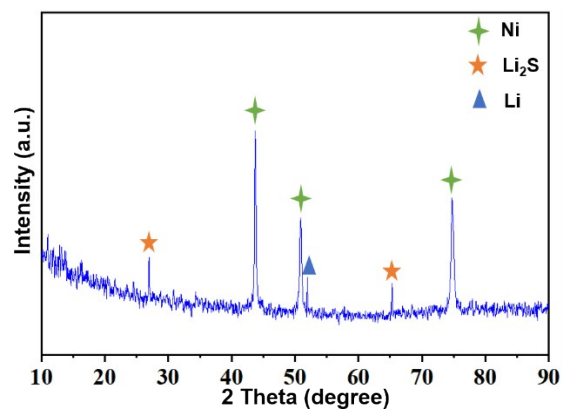


**Fig. S4.** XRD pattern of NiNWs@Ni<sub>3</sub>S<sub>2</sub> electrode after cycling for 5 times at 1 mA cm<sup>-2</sup>, 1 mAh cm<sup>-2</sup>.

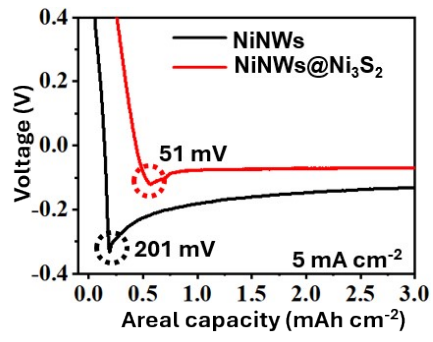


Fig. S5. The first discharge profiles of NiNWs and NiNWs@Ni<sub>3</sub>S<sub>2</sub> electrodes at 5 mA cm<sup>-2</sup>.

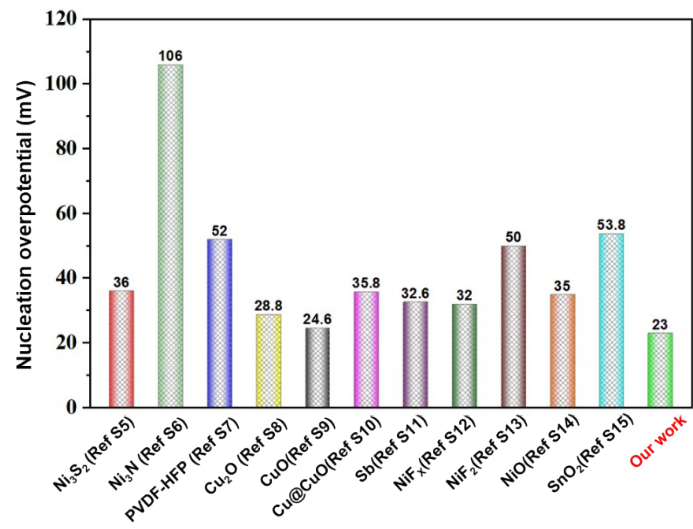
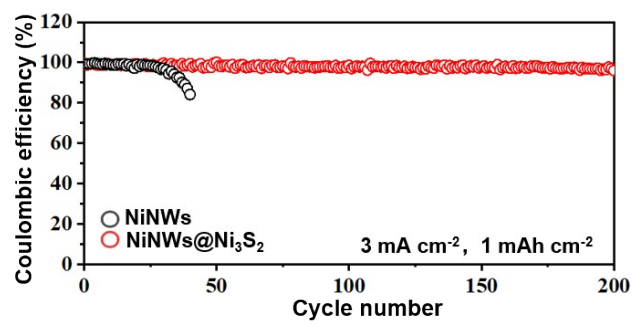
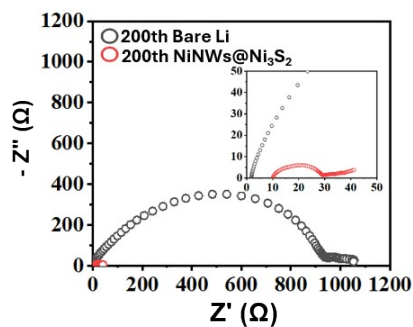


Fig. S6. Comparison of the nucleation overpotentials of our work with others at  $1 \text{ mA cm}^{-2\text{SS-15}}$ .





**Fig. S7.** CE of NiNWs and NiNWs@Ni<sub>3</sub>S<sub>2</sub> at a current density of 3 mA cm<sup>-2</sup>, 1 mAh cm<sup>-2</sup>.



**Fig. S8.** EIS plots of NiNWs and NiNWs@Ni<sub>3</sub>S<sub>2</sub> electrodes after 200 cycles at 1 mA cm<sup>-2</sup>, 1 mAh cm<sup>-2</sup> (inset is partially enlarged views at high frequency region).

The Li<sup>+</sup> diffusion coefficients were calculated using equations S2<sup>S16</sup>.

$$D_{Li^+} = R^2 T^2 / 2 A^2 n^4 F^4 C_{Li}^2 \sigma^2 \quad (S2)$$

where  $R$ ,  $A$ ,  $T$ ,  $F$ ,  $C$ ,  $n$ ,  $\omega$ , and  $\sigma$  are corresponding to the gas constant, surface area of the electrode, temperature, Faraday constant, concentration of Li<sup>+</sup>, number of electrons, frequency, and Warburg factor, respectively. The Warburg factor is displayed from  $Z'$  vs.  $\omega^{-1/2}$  diagram.

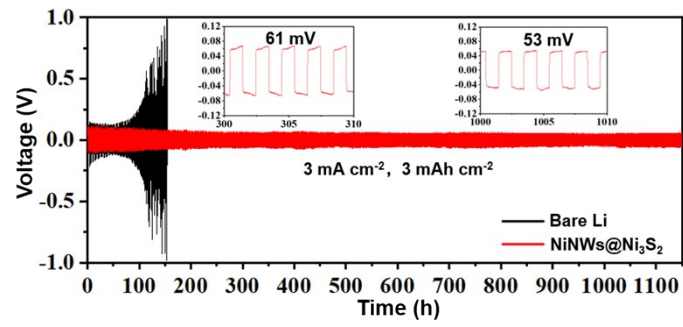


**Fig. S9.** Galvanostatic cycling voltage profile of bare Li and NiNWs@Ni<sub>3</sub>S<sub>2</sub> symmetrical cells at current densities of 3 mA cm<sup>-2</sup>, 3 mAh cm<sup>-2</sup>; insets are the magnified galvanostatic cycling voltage profiles during 300 ~ 310 h and 1000 ~ 1010 h.

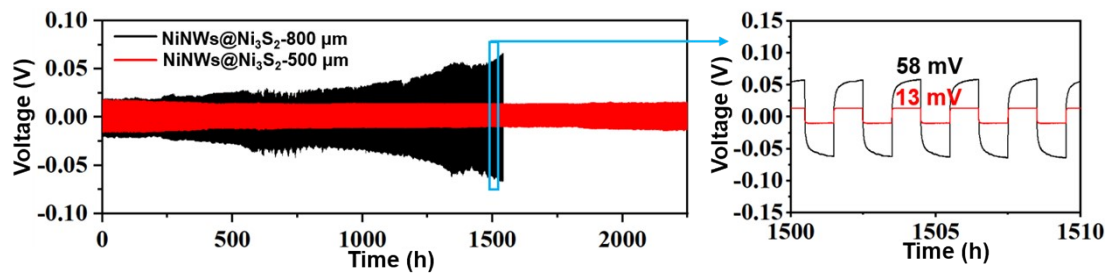


**Fig. S10.** Galvanostatic cycling voltage profile of NiNWs@Ni<sub>3</sub>S<sub>2</sub>-500 and NiNWs@Ni<sub>3</sub>S<sub>2</sub>-800 electrodes at a current density of 1 mA cm<sup>-2</sup>, 1 mAh cm<sup>-2</sup>.

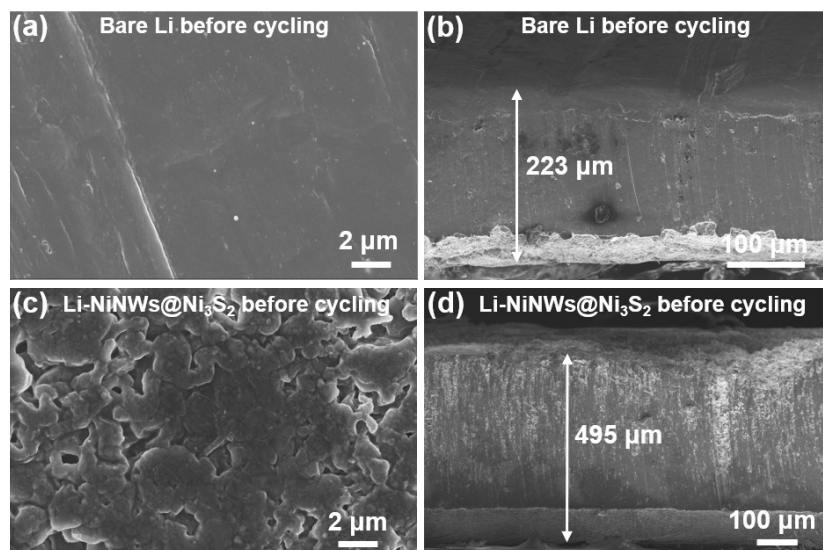


**Fig. S11.** (a) Surface and (b) cross-sectional SEM images of the Li foil electrode before cycling. (c) Surface and (d) cross-sectional SEM images of NiNWs@Ni<sub>3</sub>S<sub>2</sub> electrode before cycling.

## References

- S1. P. E. Blöchl, *Physical Review B*, 1994, **50**, 17953-17979.
- S2. K. B. John P. Perdew, Matthias Ernzerhof, *Physical Review Letters*, 1997, **77**.
- S3. S. Grimme, J. Antony, S. Ehrlich and H. Krieg, *The Journal of Chemical Physics*, 2010, **132**.
- S4. D. J. G. Kresse, *Physical Review B*, 1999, **59**.
- S5. M. Qi, L. Xie, Q. Han, X. Qiu, S. Katiyar, X. Liu, S. Yang, L. Zhu, X. Wu, L. Chen and X. Cao, *Sustainable Energy & Fuels*, 2023, **7**, 5029-5038.
- S6. L. Zhao, W. Wang, X. Zhao, Z. Hou, X. Fan, Y. Liu and Z. Quan, *ACS Applied Energy Materials*, 2019, **2**, 2692-2698.
- S7. H. Duan, Y. You, G. Wang, X. Ou, J. Wen, Q. Huang, P. Lyu, Y. Liang, Q. Li, J. Huang, Y.-X. Wang, H.-K. Liu, S. X. Dou and W.-H. Lai, *Nano-Micro Letters*, 2024, **16**.
- S8. Q. Zhang, J. Luan, Y. Tang, X. Ji, S. Wang and H. Wang, *Journal of Materials Chemistry A*, 2018, **6**, 18444-18448.
- S9. T. Gao, D. Xu, Z. Yu, Z.-H. Huang, J. Cheng and Y. Yang, *Journal of Alloys and Compounds*, 2021, **865**.
- S10. J. Luan, Q. Zhang, H. Yuan, D. Sun, Z. Peng, Y. Tang, X. Ji and H. Wang, *Advanced Science* 2019, **6**, 1901433.
- S11. X. Fu, C. Shang, G. Zhou and X. Wang, *Journal of Materials Chemistry A*, 2021, **9**, 24963-24970.
- S12. G. Huang, S. Chen, P. Guo, R. Tao, K. Jie, B. Liu, X. Zhang, J. Liang and Y.-C. Cao, *Chemical Engineering Journal*, 2020, **395**.
- S13. W. Hou, S. Li, J. Liang, B. Yuan and R. Hu, *Electrochimica Acta*, 2022, **402**.
- S14. W. Lu, C. Wu, W. Wei, J. Ma, L. Chen and Y. Chen, *Journal of Materials Chemistry A*, 2019, **7**, 24262-24270.
- S15. J.-r. Wang, M.-m. Wang, X.-d. He, S. Wang, J.-m. Dong, F. Chen, A. Yasmin and C.-h. Chen, *ACS Applied Energy Materials*, 2020, **3**, 7265-7271.
- S16. G. Henkelman, B. P. Uberuaga and H. Jónsson, *The Journal of Chemical Physics*, 2000, **113**, 9901-9904.